Diverse Functional Properties of Wilson Disease ATP7B Variants

Huster, Dominik ; Kühne, Angelika ; Bhattacharjee, Ashima ; Raines, Lily ; Jantsch, Vanessa ; Noe, Johannes ; Schirrmeister, Wiebke ; Sommerer, Ines ; Sabri, Osama ; Berr, Frieder ; Mössner, Joachim ; Stieger, Bruno ; Caca, Karel ; Lutsenko, Svetlana

Abstract: BACKGROUND AIMS: Wilson disease is a severe disorder of copper metabolism caused by mutations in ATP7B, which encodes a copper-transporting adenosine triphosphatase. The disease presents with a variable phenotype that complicates the diagnostic process and treatment. Little is known about the mechanisms that contribute to the different phenotypes of the disease. METHODS: We analyzed 28 variants of ATP7B from patients with Wilson disease that affected different functional domains; the gene products were expressed using the baculovirus expression system in Sf9 cells. Protein function was analyzed by measuring catalytic activity and copper ((64)Cu) transport into vesicles. We studied intracellular localization of variants of ATP7B that had measurable transport activities and were tagged with green fluorescent protein in mammalian cells using confocal laser scanning microscopy. RESULTS: Properties of ATP7B variants with pathogenic amino-acid substitution varied greatly even if substitutions were in the same functional domain. Some variants had complete loss of catalytic and transport activity, whereas others lost transport activity but retained phosphor-intermediate formation or had partial losses of activity. In mammalian cells, transport-competent variants differed in stability and subcellular localization. CONCLUSIONS: Variants in ATP7B associated with Wilson disease disrupt the protein's transport activity, result in its mislocalization, and reduce its stability. Single assays are insufficient to accurately predict the effects of ATP7B variants the function of its product and development of Wilson disease. These findings will contribute to our understanding of genotype-phenotype correlation and mechanisms of disease pathogenesis.

DOI: https://doi.org/10.1053/j.gastro.2011.12.048

Diverse Functional Properties of Wilson Disease ATP7B Variants

Dominik Huster, Angelika Kühne, Ashima Bhattacharjee, Lily Raines, Vanessa Jantsch, Johannes Noe, Wiebke Schirrmeister, Ines Sommerer, Osama Sabri, Frieder Berr, Joachim Mossner, Bruno Stieger, Karel Caca, Svetlana Lutsenko

PII: S0016-5085(12)00016-9
DOI: 10.1053/j.gastro.2011.12.048
Reference: YGAST 57526

To appear in: *Gastroenterology*

Received date: 27 March 2011
Revised date: 19 December 2011
Accepted date: 26 December 2011

Please cite this article as: Huster, D., Kühne, A., Bhattacharjee, A., Raines, L., Jantsch, V., Noe, J., Schirrmeister, W., Sommerer, I., Sabri, O., Berr, F., Mossner, J., Stieger, B., Caca, K., Lutsenko, S., Diverse Functional Properties of Wilson Disease ATP7B Variants, *Gastroenterology* (2012), doi: 10.1053/j.gastro.2011.12.048.

DIVERSE FUNCTIONAL PROPERTIES OF WILSON DISEASE ATP7B VARIANTS

Short title: ATP7B function and human mutations

Authors: Dominik Huster[1,2,3], Angelika Kühne[1], Ashima Bhattacharjee[4], Lily Raines[4], Vanessa Jantsch[1], Johannes Noe[5], Wiebke Schirrmeister[2,6], Ines Sommerer[1], Osama Sabri[7], Frieder Berr[1,8], Joachim Mossner[1], Bruno Stieger[5], Karel Caca[1,9,#], Svetlana Lutsenko[4#]

[1]Department of Medicine, Dermatology and Neurology, Division of Gastroenterology and Rheumatology, University of Leipzig, Leipzig, Germany

[2]Department of Gastroenterology, Hepatology and Infectious Diseases, Otto-von-Guericke-University, Magdeburg, Germany

[3]Department of Gastroenterology and Oncology, Deaconess Hospital Leipzig, Germany

[4]Department of Physiology, Johns Hopkins University, Baltimore, MD, USA

[5]Department of Clinical Pharmacology and Toxicology University Hospital Zurich, Switzerland

[6]Institute of Medical Physics and Biophysics, University of Leipzig, Germany

[7]Department of Nuclear Medicine, University of Leipzig, Germany

[8]Department of Internal Medicine, Paracelsus Medical University, Salzburg, Austria

[9]Department of Gastroenterology, Medizinische Klinik I, Klinikum Ludwigsburg

[#]Both authors contributed equally to this work.

Grant support: This work was funded by the Deutsche Forschungsgemeinschaft (HU 932/3-1), and National Institute of Health grant R01 DK071865-06 to SL.

Abbreviations used in this paper: ER, endoplasmic reticulum; TGN, trans-Golgi network; WD, Wilson disease; wt, wild-type

Corresponding author: Dominik Huster, MD, Department of Gastroenterology and Oncology, Deaconess Hospital Leipzig, Georg-Schwarz-Str. 49, 04177 Leipzig, Germany, Email: dominik.huster@diako-leipzig.de, Tel: +49 341 444 3622, Fax: +49 341 444 3623

Disclosures: The authors disclose no conflicts.

Author Contributions-List:

DH: study concept and design; acquisition of data; analysis and interpretation of data; drafting of the manuscript; critical revision of the manuscript for important intellectual content; statistical analysis; obtained funding, study supervision

AK: acquisition of data; analysis and interpretation of data; critical revision of the manuscript

AB: acquisition of data; analysis and interpretation of data; critical revision of the manuscript

LR: acquisition of data; analysis and interpretation of data; critical revision of the manuscript

VJ: acquisition of data; analysis and interpretation of data; critical revision of the manuscript

JN: study concept and design; analysis and interpretation of data; critical revision of the manuscript, technical support

WS: acquisition of data; analysis and interpretation of data; critical revision of the manuscript

IS: acquisition of data; analysis and interpretation of data; critical revision of the manuscript

OS: acquisition of data; analysis and interpretation of data; critical revision of the manuscript for important intellectual content; administrative, technical, and material support

FB: study concept and design; analysis and interpretation of data; critical revision of the manuscript for important intellectual content

JM: analysis and interpretation of data; critical revision of the manuscript for important intellectual content; obtained funding; administrative, and material support; study supervision

BS: study concept and design; analysis and interpretation of data; critical revision of the manuscript; technical, and material support

KC: study concept and design; analysis and interpretation of data; critical revision of the manuscript for important intellectual content; administrative, and material support; study supervision

SL: study concept and design; analysis and interpretation of data; drafting of the manuscript; critical revision of the manuscript for important intellectual content; statistical analysis; obtained funding; administrative, technical, or material support; study supervision

Abstract

BACKGROUND & AIMS: Wilson disease is a severe disorder of copper metabolism caused by mutations in *ATP7B*, which encodes a copper-transporting ATPase. The disease presents with a variable phenotype that complicates the diagnostic process and treatment. Little is known about the mechanisms that contribute to the different phenotypes of the disease. **METHODS:** We analyzed 28 variants of *ATP7B* from patients with Wilson disease that affected different functional domains; the gene products were expressed using the baculovirus expression system in Sf9 cells. Protein function was analyzed by measuring catalytic activity and copper (^{64}Cu) transport into vesicles. We studied intracellular localization of variants of ATP7B that had measurable transport activities and were tagged with green-fluorescent protein in mammalian cells using confocal laser scanning microscopy. **RESULTS:** Properties of ATP7B variants with pathogenic amino-acid substitution varied greatly even if substitutions were in the same functional domain. Some variants had complete loss of catalytic and transport activity, whereas others lost transport activity but retained phospho-intermediate formation or had partial losses of activity. In mammalian cells, transport-competent variants differed in stability and subcellular localization. **CONCLUSIONS: Variants in ATP7B associated with Wilson disease disrupt the protein's transport activity, result in its mis-localization, and reduce its stability. Single assays are insufficient to accurately predict the effects of *ATP7B* variants the function of its product and development of Wilson disease. These findings will contribute to our understanding of genotype–phenotype correlation and mechanisms of disease pathogenesis.**

KEY WORDS: P-type ATPase; genetic analysis; liver disease; Golgi

Wilson disease (WD) is a hereditary disease due to mutations of the copper transporting P-type ATPase *ATP7B*. WD is associated with copper accumulation resulting in liver damage and/or neurologic symptoms[1,2]. The manifestations of liver disease vary from clinically asymptomatic with only biochemical abnormalities to acute liver failure[3]. Similarly, the spectrum of neurologic manifestations ranges from normal or mild disturbances to a rapid and severe progression of neurologic disability[4]. The mechanisms behind this variability are likely to be complex because even monozygotic twins may have different disease manifestations[5]. Genetic studies showed some association between several mutations and the age of onset/disease severity[6-9]; however, robust genotype-phenotype correlation in the case of missense mutations has not so far been found, although complete loss of protein expression due to non-sense mutations is expected to result in a more severe phenotype. This study focuses on one potential source of phenotypic variability – the effect of mutations in *ATP7B* on the function of the corresponding Cu-transporting Wilson ATPase.

To date, more than 500 different mutations associated with WD are known (http://www.wilsondisease.med.ualberta.ca/database.asp)[10]. The high prevalence of compound heterozygosity prevents a clear correlation between genotype and phenotype in affected individuals. A large fraction of mutations are missense mutations producing a single amino-acid change in Wilson ATPase ATP7B. ATP7B is a large membrane protein located in the *trans*-Golgi network (TGN). In normal liver, ATP7B has two functions: (i) it transports copper into the TGN for incorporation into ceruloplasmin and (ii) exports excess copper by sequestering metal in vesicles for subsequent biliary excretion. The second function requires ATP7B trafficking from TGN to endocytic vesicles in response to elevation of intracellular copper concentration.

The ATP7B-mediated transport of copper involves several steps. First, ATP7B binds copper via its cytosolic N-terminal domain and ATP via the nucleotide-binding domain. ATP is then hydrolyzed, and ATP7B becomes transiently phosphorylated at the residue D1027 located in the P-domain (catalytic phosphorylation). Subsequent dephosphorylation releases energy necessary to transfer copper across membrane (transport step) (Figure 1A,B). Each of these steps may be affected by WD-causing mutations[11]. The effect could be severe resulting in a complete loss of ATP7B function, if mutated residues are critical for binding of ATP or copper and/or conformational transitions during catalysis. The inactivation of ATP7B could also be partial if mutations diminish affinity for substrates, slow down conformational transitions or interfere with precise protein targeting to TGN or vesicles. Understanding of phenotypic diversity in WD requires knowledge of how causative mutations alter protein stability, activity, and localization in the cell.

Presently, for most of the WD-causing mutations, such detailed information is not available. Yeast complementation assay was used to segregate ATP7B mutants into “severe” and “mild” categories based on their ability to restore the growth of yeast strain that lacks the endogenous copper transporter[12-14]. Studies in mammalian cells revealed decreased protein levels and mislocalization for several mutants[15-17] with a surprisingly small effect on copper transport, which was evaluated indirectly[17]. So far, no studies have directly assessed the transport or catalytic activity of disease-causing mutants. Such information is necessary for future mechanism-based attempts to correct the ATP7B function. Here, we directly measured catalytic and transport activity of 28 ATP7B variants representing all protein domains (Table 1, Figure 1B) and tested the intracellular localization for mutants, for which transport activity was observed. The mutants and variants were chosen based on clinical findings (see WD database[10]) and recent literature; gene variants found in the population with no WD symptoms were also characterized.

Materials and Methods

Reagents and cell lines

All chemicals, unless otherwise specified, were purchased from Sigma (Deisenhofen, Germany). Sf9 cells (Invitrogen, Carlsbad, CA) were maintained at 27°C in suspension cultures in Sf-900 II (Gibco, Grand Island, NY). HEK293 T-REx™ cells (Invitrogen, Carlsbad, CA) were maintained at 37^{o}C in adherent cultures in MEM (Gibco, Carlsbad, CA) media with 10% FBS, 3% penicillin-streptomycin, 1% non-essential amino acids, 0.1% zeocin, and 0.1% blasticidin.

Generation of Recombinant Baculovirus ATP7B variants

The plasmid encoding the full-length 4.4-kilobase ATP7B cDNA (pFastBacDual-wt-ATP7B) and the catalytically inactive D1027A mutant were previously described[18] and used as a template. The ATP7B mutations were introduced with the QuikChange^{TM} site-directed mutagenesis kit (Stratagene, La Jolla, CA) and appropriate primers (Supplementary Table 1). The entire coding sequence of all constructs was verified by automated sequencing.

Expression in Sf9 insect cells and preparation of membrane fractions

Maintenance, infection with recombinant viruses, harvesting of *Sf9* insect cells, and isolation of membrane fractions were carried out as described earlier[18,19]. To obtain a total microsomal fraction, cells from a 50-ml culture were pelleted by centrifugation at 500*g* (10 min, 4°C) and then resuspended in 5 ml of homogenizing buffer (HB): 25 mM imidazole, pH 7.4, 0.25 M sucrose, 1 mM dithiothreitol (DTT), 1 mM 4-(2-Aminoethyl)benzenesulfonyl fluoride hydrochloride (AEBSF). One tablet of complete protease inhibitor mixture without EDTA (Roche, Basel, Switzerland) was added per 50 ml of buffer solution. Cells were homogenized by 20 strokes in a Dounce glass homogenizer, and then centrifuged (10 min,

500*g)*. The supernatant was subjected to an additional centrifugation (30 min, 20000*g*) to pellet microsomal membranes, that were then resuspended in HB-buffer and stored at -80°C. Protein concentration in membrane fraction was determined by the method of Lowry[20]. The expression of wt- and mutant ATP7B was analyzed by separating 50 µg total membrane protein on a 7.5% Laemmli gel[21] followed by Coomassie staining and Western blotting with polyclonal antibody a-ABD (1:20,000)[18,19].

Preparation of vesicles for copper transport

Sf9 cells were infected with virus encoding wt-ATP7B, empty vector (mock), or ATP7B variants and harvested after three days. Cells from a 50 ml culture were pelleted, resuspended in 6 ml of ice-cold buffer containing 50 mM Tris, pH 7.0, 50 mM mannitol, 2 mM ethylene glycol-bis-(2-aminoethyl)-N,N,N', N'-tetraacetic acid, antipain and leupeptin (each diluted 1:1000), phenylmethylsulfonyl fluoride (diluted 1:200), homogenized 20x in a semi-automatic homogenizer (Schütt homgen plus, Göttingen, Germany) at 3000 rpm, and then centrifuged (10 min, 500*g*, 4°C). Subsequently, the supernatant was centrifuged (1 h, 100000*g*) to sediment the membranes. The membranes were resuspended in a sterile filtered buffer (SMS): 50 mM sucrose, 100 mM potassium nitrate, 10 mM Hepes/Tris pH 7.4. Vesicle formation was facilitated by vortexing and passing several times through a 25-gauge 5/8-inch needle. The vesicles were stored in liquid nitrogen. Protein concentration was determined by the method of Bradford[22]. To confirm protein expression, all samples were analyzed by Western analysis using polyclonal antibody a-ABD[18,19].

^{64}Cu-uptake in vesicles

The transport assay was performed according to Gmaj *et al.*[23]. The vesicle solution was thawed, diluted to 5 µg protein/µl with sterile filtered SMS buffer and kept on ice until further use. For the transport assay, 20 µl vesicle solution was pre-incubated at 37°C for 1 min. The

reaction was started at 37°C by addition of 80 µl sterile filtered radioactive incubation solution: 50 mM sucrose, 100 mM KNO_3, 10 mM Hepes/Tris pH 7.4, 12.5 mM $Mg(NO_3)_2$, 12.5 mM DTT, 6.25 mM ATP, 2.5 µM $CuCl_2$ (final copper concentration 2 µM), 6 µCi/ml ^{64}Cu (Rotop Pharmaka, Radeberg, Germany). For inhibition experiments, orthovanadate was added to the incubation solution to a final concentration of 200 µM. The copper transport reaction was stopped after 2 min, 5 min, 20 min 45 min, 120 min or 240 min by addition of 3 ml of ice-cold sterile filtered stopping solution (50 mM sucrose, 100 mM KCl, 10 mM Hepes/Tris pH 7.4, 0.5 mM EDTA) and filtered immediately through a 0.45 µm nitrocellulose-vacuum-filter-system. The filter was washed with 3 ml stopping solution before and after filtration and its radioactivity was measured by the γ-Counter Cobra Quantum (PerkinElmer, Rodgau-Jügesheim, Germany). To measure the background radioactivity, 3 ml stopping solution was added to the vesicle solution on ice prior to the addition of 80 µl incubation solution. Vesicles with an empty vector (mock) and inactive variant D1027A were used as negative controls. The data were analyzed by a nonlinear regression using SigmaPlot software.

[γ-^{32}P]ATP-phosphorylation

Membrane preparations (50 µg) containing wt-ATP7B or mutants were resuspended in 200 µl phosphorylation buffer: 20 mM bis-Tris propane, pH 7, 200 mM KCl, 5 mM $MgCl_2$. Radioactive [γ-^{32}P] ATP (5 µCi, specific activity 20 mCi/µmol, PerkinElmer, Waltham, MA) was added to a final concentration of 1 µM and the mixture was incubated on ice for 4 min. The reaction was stopped by addition of 50 µl of ice-cold 1 mM NaH_2PO_4 in 50% trichloroacetic acid and then centrifuged (10 min, 20000*g*). The protein pellet was washed once with 1 ml ice-cold water and centrifuged a second time for 5 min. The pellet was dissolved in 40 µl sample buffer (5 mM Tris-PO_4, pH 5.8, 6.7 M urea, 0.4 M DTT, 5% SDS,

Bromphenol blue) and 30 µl were loaded on a 7% acidic gel (stacking gel: 5.5% acrylamide, 41.3 mM TRIS, pH 5.8, 1% SDS, 5% ammonium persulfate, 5% TEMED; separating gel: 7% acrylamide, 64.5 mM TRIS, pH 6.8, 1% SDS, 6,25% ammonium persulfate, 6.25% TEMED). After electrophoresis the gels were fixed in 10% acetic acid for 10 min and dried on blotting paper. The dried gels were exposed overnight either to a screen for the Fuji BAS reader (Fuji, Düsseldorf, Germany) or Kodak BioMax MR film (Kodak, Rochester, NY). The photon-stimulated-luminescence intensity of bands was quantified using Aida Image Analyzer (Raytest, Straubenhardt, Germany). To test ATP-dependent dephosphorylation, ATP was added after [γ-^{32}P]ATP phosphorylation to a final concentration of 1 mM at room temperature and incubated for 10 min before the reaction was stopped and samples were processed in the same manner as described above.

Expression and localization of ATP7B variants in HEK 293 T-REx™ cells

Selected mutations (L1083F, R969Q, and A874V) were introduced into a GFP-ATP7B construct (kindly provided by Dr. Ann Hubbard, Johns Hopkins University) using the QuikChange Site Directed Mutagenesis kit and appropriate primers (Supplementary Table 1). The presence of the desired mutation and the absence of additional mutations were confirmed by DNA sequencing. For transfection into mammalian cells, plasmids were isolated using a Zyppy™ Endo-free Plasmid Miniprep Kit (Zymo Research, Irvine, CA). HEK 293 TREx™ cells were seeded on flame-sterilized coverslips in twelve-well plates and allowed to grow until approximately 70-80% confluency. Transfections of 2500 ng of plasmid DNA were performed in a serum free MEM media for 6 hours using 4 µL of TurboFect™ reagent (Fermentas, Glen Burnie, MD) per well. The media was then replaced with Gibco MEM media (with 10% FBS, 3% penicillin-streptomycin, 1% non-essential amino acids) and

left overnight at 37°C or 28°C. Cells were fixed with chilled 1:1 aceton:methanol mixture for 30 seconds and blocked overnight in blocking buffer (1% gelatin, 1% BSA in PBS).

Primary antibody solutions were prepared by diluting into blocking buffer with 0.1% Tween. Dilutions were as follows: TGN38 (H-300) Rabbit Polyclonal Antibody (Santa Cruz Biotech, Santa Cruz, CA), 1:150; Sheep Antibody to Human TGN46 (GeneTex, Irvine, CA), 1:150; Rabbit anti-Calnexin C-terminus (Enzo Life Sciences, Plymouth Meeting, PA), 1:500, 1:250, 1:150. Sixty µl of each antibody solution was aliquoted on Parafilm within a humidifying chamber for each coverslip. Coverslips were placed onto these primary antibody solutions cell side down and kept at room temperature for two hours. After two 5-minute washes with PBS and two 5-minute washes with PBST (0.5% Tween in PBS), coverslips were treated with a secondary antibody for one hour and protected from light. Following dilutions were used: Alexa Fluor 555 goat anti-rabbit IgG (Invitrogen, Carlsbad, CA), 1:500; Alexa Fluor 555 donkey anti-sheep IgG (Invitrogen, Carlsbad, CA), 1:250. Two PBS washes, three PBST washes, and a final PBS wash were done to remove unbound antibody. Slides were rinsed in Milli-Q® purified water to remove residual salts, then mounted with Vectashield Mounting Medium (Vector Laboratories, Burlingame, CA) with DAPI and visualized using a Zeiss LSM 5 Pascal confocal microscope with a 100·objective lens (Carl Zeiss AG, Oberkochen, Germany).

Protein modeling

The location of the mutations in different functional domains was visualized using available NMR structures for the N-domain[24], N-terminal Cu-binding unit domain[25] and the A-domain[26]. The structures of the P-domain where modeled using the ESyPred3D Web Server 1.0 and the crystallographic structures of CopA ATP-binding domain as template (RCSB accession number 2b8e)[27,28].

Results

In vitro copper transport assay

We first determined whether an ATP7B-dependent copper transport can be detected in ATP7B-containing microsomal vesicles from Sf9 cells used as a model for TGN vesicles. In the presence of ATP, the addition of ^{64}Cu resulted in an accumulation of copper in ATP7B-containing vesicles (Figure 2); whereas no transport was observed in vesicles prepared from cells infected with empty virus (mock) (Figure 2A). To verify that copper accumulation was due to an enzymatically-driven process, we repeated experiments at 4°C. No copper accumulation was observed at 4°C (Figure 2A). Orthovanadate (200 μM Na_3VO_4), a general inhibitor of P-type ATPases, significantly inhibited but did not fully eliminate copper uptake (Figure 2A). Consequently, to further verify that copper accumulation was due to transport and not simply binding of copper to ATP7B, we analyzed the D1027A mutant of ATP7B, in which catalysis is disrupted but copper binding is preserved. This mutant yielded no copper accumulation in vesicles (Figure 2B).

The effect of mutations on copper transport

To determine the effect of mutations on ATP7B transport function, we generated 25 WD-associated variants and three predicted polymorphisms. Substitutions were made within different functional domains to better understand the structure-function relationships (Figure 1B). The wt-ATP7B and mutants were expressed in the *Sf9* cells under identical conditions. Western blot analysis illustrated that protein expression was easily detectable for all mutants (Supplementary Figure 1). In contrast, there was a marked variation in copper transport (Table 1, Figure 2C,D, Supplementary Figure 2). The majority of ATP7B mutants (16 out of total 25) had essentially no activity (less than 5% of wt) or a very low activity (5-10%); the H1069Q mutant (frequently found in Caucasian population) belonged to this latter category

(Figure 2C). Unexpectedly, a sizeable fraction (8 out of 25) of mutants showed partial transport activity (0.22-0.71 nmol/mg protein at 120 min). These mutants included A874V (frequently detected in Korean population[29]) and I857T. Most of the partially active mutants had slower transport rates and accumulated less copper than the wt-ATP7B, except the S406A variant that had a slower rate compared to the wt but with time yielded the same level of copper accumulation in vesicles (Figure 2C,D). Only one of the ATP7B mutants, M645R, displayed Cu-uptake (1.18 nmol/mg protein at 120 min) indistinguishable from wt-ATP7B (Figure 2C). The predicted non-disease variants (V456L and K832R) also showed reduced transport rates (Figure 2D). To further verify that these marked variations in activity were not simply due to differences in ATP7B expression levels, we selected several mutants that had similar transport activity, expressed them in parallel under identical conditions, and quantified ATP7B amounts by densitometry. Supplementary Figure 3 illustrates that a drastically different activity of these mutants is not due to difference in their expression levels.

Effect of mutations on catalytic activity

The loss of copper transport could be either due to disruption of copper transfer across membranes or due to the loss of ATP binding/hydrolysis. To better understand which of the steps is affected, we examined the ability of ATP7B to form a phosphorylated intermediate upon ATP binding (Figure 3, Table 1). In all A-domain mutants phosphorylation was markedly increased (Figure 3C). This result indicated that ATP-binding is unaltered, but the well-known function of the A-domain to facilitate dephosphorylation[11] was inhibited. In contrast, ATP7B variants with mutations in the N-terminal domain (Figure 3A), transmembrane domain (Figure 3B), the P- or N-domains (Figure 3D, and E respectively) showed either normal or reduced phosphorylation. All three *ATP7B* gene variants not

associated with disease showed normal phosphorylation activity (Figure 3F). Thus, in our subset of mutants, disruption of ATP binding is not a major defect.

Partial transport activity along with hyperphosphorylation for several mutants suggested that these mutants have altered conformation (or defects in the communication between functional protein domains necessary for optimal protein activity). This conclusion was supported by experiments on dephosphorylation. When hyperphosphorylated mutants were incubated with cold ATP, dephosphorylation was observed for all examined mutants (Figure 4A,B). Thus, the hyperphosphorylated mutants are able to perform all the steps of the cycle and the transport defect in these mutants is associated with structural changes affecting rates of the individual step(s).

Expression and localization of functional ATP7B mutants in mammalian cells

The ability of several mutants to hydrolyze ATP and transport copper *in vitro* suggested that in cells their properties can further be altered exacerbating the phenotype. To test this hypothesis, three transport competent mutants (found in different domains: A-domain (A874V), N-domain (L1083F) and in the trans-membrane domain (R969Q)) were produced as GFP-tagged versions and their expression and localization were examined in mammalian cells. The R969Q variant showed fluorescent intensity similar to that of the wt-ATP7B and normal intracellular targeting, as illustrated by co-localization with the TGN marker TGN46 (Figure 5). In contrast, L1083F and A874V showed significant abnormalities in their sub-cellular localization and protein levels. When expressed at 37°C, L1083F and A874V displayed characteristic endoplasmic reticulum (ER) localization, which was confirmed by co-staining with the ER marker Calnexin (Figure 5). Both mutants also showed weaker signal intensity compared to wt-ATP7B. Thus, despite the lack of gross misfolding (indicated by the ability to perform key functional reactions *in vitro*), the structural changes in A874V and

L1083F mutants were sufficient to produce apparent destabilization and ER retention. Thus, mislocalization is the major reason for the loss of copper delivery to the TGN by these mutants.

Previous studies reported that the stability and localization of some ATP7B mutants (e.g. R778L and H1069Q) can be corrected by growing cells at 30°C[17]. Consequently, we tested whether the targeting of A874V and L1083F (which show copper transport activity after being expressed at 27°C in Sf9 cells (Table 1, Supplementary Figure 2B,D)) can be corrected by lowering temperature during expression. For A874V no improvement in either protein levels or targeting was seen in mammalian cells maintained at 28°C (attempts to stabilize this mutant by growing cells with increasing copper concentrations were also unsuccessful, data not shown). For the L1083F mutant, some TGN localization could be detected, but cold temperature alone was insufficient to induce TGN targeting (Supplementary Figure 4).

Discussion

ATP7B variants have a wide spectrum of properties. In this study we have investigated the effect of WD-causing mutations on the functional activity and intracellular functionality of ATP7B. Utilization of a heterologous expression system and membrane vesicles allowed us for the first time to directly evaluate the transport activity of a large set of clinically relevant mutants. Our results indicate that a significant diversity already exists at the molecular level, as the mutants display a markedly different stability, localization, catalytic, and transport activity. Therefore, detailed characterization of each WD-causing mutant may be necessary for better understanding of the genotype-phenotype correlations in WD. Although mutations located in the same domain may have similar properties (for example, we detected increased levels of phospho-intermediate in the A-domain mutants), the localization in a

certain domain alone is not predictive of the properties of a mutant. This conclusion can be illustrated by different transport characteristics of the P840L and I857T, both situated in the A-domain (Figure 6A). The more severe effect of P840L on protein function is likely due to a more disruptive nature of Pro>Leu substitution (replacing a small and kink-inducing Pro residue with a bulky and hydrophobic Ile) compared to replacement of Ile with a smaller Thr.

The comparison of A874V with the recently characterized G875R variant further illustrates an extremely delicate and precise architecture of the ATP7B molecule[30]. The A874V mutation is located within the flexible loop of the A-domain (Figure 6A) and is not expected to markedly alter protein structure. This prediction is consistent with the actual functional properties of the mutant, i.e. its ability to transport copper using ATP hydrolysis. And yet, in cells the lack of precise folding prevents the A874V exit from the ER, thus disrupting copper delivery to the secretory pathway and likely causing WD phenotype. Similar ER retention of G875R (the mutation of a neighboring residue) can be corrected by increasing copper concentration in cells[30], which facilitates ER exit and proper TGN targeting (and activity). In contrast, treatment with copper does not improve the A874V stability or localization. Altogether, our studies demonstrate the need for utilizing an arsenal of methods for understanding the phenotype of disease-causing mutation, since individual assays yields only partial and non-overlapping information about ATP7B properties.

It is useful to compare the advantages and disadvantages of various assays and information that can be generated. Yeast complementation assay is an effective way to identify ATP7B mutants, which completely lost their transport activity from those that have some activity left[12]. However, it is difficult to draw more specific conclusions about properties of the WD mutants because it is unknown how much copper transport activity is necessary to allow yeast to grow. Overexpression of mutants with very low activity might be sufficient to allow

copper delivery to the TGN and growth. In addition, yeast cells grow at lower temperature (30^{o}C), which may be sufficient to stabilize proteins that unfold and degrade at 37^{o}C. For example, H1069Q, which has low copper transport activity and is unstable in mammalian cells[13] complements yeast phenotype[31]

Expression in insect cells may underestimate the effects of mutation on protein stability due to lower temperature necessary for growth of insect cells (27°C). However, it provides a marked advantage when detailed mechanistic understanding of functional consequences of mutations is desirable. We found that measurements of catalytic phosphorylation and dephosphorylation of ATP7B mutants expressed in Sf9 cells were the least predictive of the overall functional outcome of mutations as many mutants that showed no transport activity were still able to undergo catalytic phosphorylation. Since the phosphorylation assay is least sensitive, we suggest that the mutants that show no activity in this assay are most severely affected. Indeed, these mutants (G85V, L492S, G1266R, E1046K, and D1222V) show neither catalytic nor transport activity. The marked effect of the last three mutations on ATP hydrolysis is not surprising as they all affect conserved residues in the immediate vicinity to ATP (Figure 6A). In contrast, dramatic negative effects of G85V and L492S mutants were unexpected as both residues belong to the regulatory N-terminal domain, which is thought not to be critical for ATP binding and hydrolysis. We hypothesize that these mutants may mediate their effect indirectly through interaction with other functional domains. Because the N-domain interacts with the ATP-binding domain and these interactions affect protein activity[32], abnormal inter-domain interaction due to mutation may decrease affinity for ATP and/or trap protein in conformation not suitable for ATP hydrolysis.

The transport assay is the most direct way to evaluate ATP7B function. This assay identified several mutants that were transport competent, i.e. could be functional in a cell. Identification

of such mutants is particularly important, because they are promising candidates for possible corrective therapy. Such variants include M769V, I857T, A874V, all located in the A-domain, (Figure 6A, left). Unlike mutations in the P- and N-domains (Figure 6A middle, right), there residues are not involved in the formation of the substrate binding sites and their substitution is more likely to alter protein stability or targeting. As described above, characterization of one of this mutant A874V revealed limitations of the *in vitro* assays (and possibly all heterologous systems) in predicting the mutant phenotype in mammalian cells. In mammalian cells at either 28°C or 37°C, A874V has the ER localization and low expression pointing to significant instability of this mutant. Such instability was not detected in insect cells suggesting that mammalian cells have much more sensitive protein quality control.

Combination of the in vitro and in vivo assays also discriminates between the effects of mutations on protein folding and function. Protein stability in cells is not indicative of function, because catalytically inactive mutants could be structurally stable, whereas partially active mutants may degrade rapidly, producing a "complete-loss of function" phenotype. Having information on both parameters could be particularly important for future attempts to correct the mutant phenotype by improving protein stability. For example, increasing stability of mutants such as the A874V mutant could be beneficial, because A874V has a significant transport activity. Recent studies using pharmacological folding chaperones 4-phenylbutyrate and curcumin illustrate a possibility of correcting the stability/folding defects of several ATP7B mutants in cells[17]. In contrast, improving stability of other mutants (such as G85V or mutants located in the vicinity of the key functional sites, Figure 6A) can be without effect since these mutants lack catalytic and transport activity. Lastly, our studies revealed that the non-disease causing changes (V456L and K832R) may nevertheless decrease ATP7B activity. Thus presence of such variants, while by itself no causative, may have a

compound effect when found in combination with other mutations and put carriers at disadvantage.

In conclusion, mutations in *ATP7B* have various effects altering protein expression levels, catalytic and transport activity, as well as intracellular localization (Figure 6B). Mutants with a partial preserved transport function may result in later onset of disease or have variable manifestation if their stability and localization is modulated by the metabolic state of cells. Detailed characterization of ATP7B mutants is likely to contribute to the analysis of genotype-phenotype correlations in WD.

Acknowledgements

The authors thank L. Thiel and Dr. R. Schliebs (University of Leipzig, Germany) and Dr. N. Taudte (Martin-Luther-University of Halle, Germany) for advice with experimental design and technical assistance. K.C. and S.L. contributed equally to this work.

References

1. Pfeiffer RF. Wilson's Disease. Semin Neurol 2007;27:123-32.
2. Huster D. Wilson disease. Best Pract Res Clin Gastroenterol 2010;24:531-9.
3. Riordan SM, Williams R. The Wilson's disease gene and phenotypic diversity. J Hepatol 2001;34:165-171.
4. Lorincz MT. Neurologic Wilson's disease. Ann N Y Acad Sci 2010;1184:173-87.
5. Kegley KM, Sellers MA, Ferber MJ, et al. Fulminant Wilson's disease requiring liver transplantation in one monozygotic twin despite identical genetic mutation. Am J Transplant 2010;10:1325-9.
6. Czlonkowska A, Gromadzka G, Chabik G. Monozygotic female twins discordant for phenotype of Wilson's disease. Mov Disord 2009;24:1066-9.
7. Caca K, Ferenci P, Kuhn HJ, et al. High prevalence of the H1069Q mutation in East German patients with Wilson disease: rapid detection of mutations by limited sequencing and phenotype-genotype analysis. J Hepatol 2001;35:575-581.
8. Stapelbroek JM, Bollen CW, van Amstel JK, et al. The H1069Q mutation in ATP7B is associated with late and neurologic presentation in Wilson disease: results of a meta-analysis. J Hepatol 2004;41:758-63.
9. Ferenci P, Czlonkowska A, Merle U, et al. Late-onset Wilson's disease. Gastroenterology 2007;132:1294-8.
10. Kenney SM, Cox DW. Sequence variation database for the Wilson disease copper transporter, ATP7B. Hum Mutat 2007;28:1171-1177.
11. Tsivkovskii R, Purnat T, Lutsenko S. Copper-transporting ATPases: key regulators of intracellular copper concentration. In: Futai M, Wada Y, Kaplan J, eds. Handbook of ATPases. Weinheim: Wiley-VCH Verlag GmbH & Co., 2004:99-158.

12. Forbes JR, Cox DW. Functional characterization of missense mutations in ATP7B: Wilson disease mutation or normal variant? Am J Hum Genet 1998;63:1663-1674.
13. Hsi G, Cullen LM, Macintyre G, et al. Sequence variation in the ATP-binding domain of the Wilson disease transporter, ATP7B, affects copper transport in a yeast model system. Hum Mutat 2008;29:491-501.
14. Luoma LM, Deeb TM, Macintyre G, et al. Functional analysis of mutations in the ATP loop of the Wilson disease copper transporter, ATP7B. Hum Mutat 2010;31:569-77.
15. Huster D, Hoppert M, Lutsenko S, et al. Defective cellular localization of mutant ATP7B in Wilson's disease patients and hepatoma cell lines. Gastroenterology 2003;124:335-45.
16. Payne AS, Kelly EJ, Gitlin JD. Functional expression of the Wilson disease protein reveals mislocalization and impaired copper-dependent trafficking of the common H1069Q mutation. Proc Natl Acad Sci USA 1998;95:10854-10859.
17. van den Berghe PV, Stapelbroek JM, Krieger E, et al. Reduced expression of ATP7B affected by Wilson disease-causing mutations is rescued by pharmacological folding chaperones 4-phenylbutyrate and curcumin. Hepatology 2009;50:1783-95.
18. Tsivkovskii R, Eisses JF, Kaplan JH, et al. Functional properties of the copper-transporting ATPase ATP7B (the Wilson's disease protein) expressed in insect cells. J Biol Chem 2002;277:976-983.
19. Huster D, Lutsenko S. The distinct roles of the N-terminal copper-binding sites in regulation of catalytic activity of the Wilson's disease protein. J Biol Chem 2003;278:32212-8.
20. Lowry OJ, Rosebrough NJ, Farr AL, et al. Protein measurement with the Folin phenol reagent. J Biol Chem 1951;193:265-275.
21. Laemmli UK. Cleavage of structural proteins during the assembly of the head of bacteriophage T4. Nature 1970;227:680-5.

22. Kruger NJ. The Bradford method for protein quantitation. Methods Mol Biol 1994;32:9-15.
23. Gmaj P, Zurini M, Murer H, et al. A high-affinity, calmodulin-dependent Ca2+ pump in the basal-lateral plasma membranes of kidney cortex. Eur J Biochem 1983;136:71-6.
24. Dmitriev O, Tsivkovskii R, Abildgaard F, et al. Solution structure of the N-domain of Wilson disease protein: Distinct nucleotide-binding environment and effects of disease mutations. Proc Natl Acad Sci USA 2006;103:5302-7.
25. Banci L, Bertini I, Cantini F, et al. Metal binding domains 3 and 4 of the Wilson disease protein: solution structure and interaction with the copper(I) chaperone HAH1. Biochemistry 2008;47:7423-9.
26. Banci L, Bertini I, Cantini F, et al. Solution structures of the actuator domain of ATP7A and ATP7B, the Menkes and Wilson disease proteins. Biochemistry 2009;48:7849-55.
27. Sazinsky MH, Agarwal S, Arguello JM, et al. Structure of the actuator domain from the Archaeoglobus fulgidus Cu(+)-ATPase. Biochemistry 2006;45:9949-55.
28. Sazinsky MH, Mandal AK, Arguello JM, et al. Structure of the ATP binding domain from the Archaeoglobus fulgidus Cu+-ATPase. J Biol Chem 2006;281:11161-6.
29. Yoo HW. Identification of novel mutations and the three most common mutations in the human ATP7B gene of Korean patients with Wilson disease. Genet Med 2002;4:43S-48S.
30. Gupta A, Bhattacharjee A, Dmitriev O, et al. Cellular copper levels determine the phenotype of the Arg875 variant of ATP7B/Wilson disease protein. Proc Natl Acad Sci USA 2011;108:5390-5.
31. Iida M, Terada K, Sambongi Y, et al. Analysis of functional domains of Wilson disease protein (ATP7B) in Saccharomyces cerevisiae. FEBS Lett 1998;428:281-285.
32. Tsivkovskii R, MacArthur BC, Lutsenko S. The Lys1010-Lys1325 fragment of the Wilson's disease protein binds nucleotides and interacts with the N-terminal domain of this protein in a copper-dependent manner. J Biol Chem 2001;276:2234-2242.

Table 1

Copper transport and phosphorylation activity of wild-type, mutant, and variant ATP7B (A-domain: Actuator domain; NTD: N-terminal Cu-binding domain; N-domain: nucleotide-binding domain; P-domain: phosphorylation domain; TMD, transmembrane domain; see Figure 1B). Copper uptake was considered impaired (no) (<5% of wt at 120 min, 0-0.07 nmol/mg); low (5-10% of wt, 0.08-0.14 nmol/mg); partial (11-75% of wt, 0.15-0.99 nmol/mg); normal (>75% of wt, >1.0 nmol/mg). The ability to form phosphorylated intermediate (catalytic phosphorylation) was considered normal (60-140% of wt); inactive (<60% of wt); hyperphoshorylated (>140% of wt). Mutations highlighted in bold are predicted to be most severe (markedly affect copper transport or both functionalities), whereas mutations highlighted in italics are likely to be less severe or potentially correctable.

	Protein domain	Cu-uptake at 120 min (nmol/mg protein); (SD)	Transport	Phosphorylation activity (% of wt); (SD)	Activity
wt-ATP7B	-	1.33 (0.18)	normal	100.0	normal
Artificial mutant of phosphorylation site:					
D1027A	P-domain	0.04 (0.01)	no	25.6 (8.4)	inactive
Human mutants:					
G85V	NTD	0.11 (0.02)	low	27.3 (25.3)	inactive
L492S	NTD	0.11 (0.02)	low	43.6 (16.5)	inactive
R616W	NTD	0.14 (0.01)	low	223.1 (28.2)	hyperphosph.
G626A	NTD	0.28 (0.01)	partial	86.3 (37.9)	normal
M645R	NTD	1.18 (0.06)	normal	167.3 (74.5)	hyperphosph.
G710S	Loop 2-3	0.08 (0.01)	low	69.1(24.6)	normal
P760L	TMD 4	0.09 (0.07)	low	152.1 (46.8)	hyperphosph.
D765N	TMD 4	0.61 (0.02)	partial	148.0 (97.9)	hyperphosph.
M769V	TMD 4	0.65 (0.01)	partial	203.3 (32.9)	hyperphosph.
P840L	A-domain	0.08 (0.01)	low	292.9 (83.7)	hyperphosph.

I857T	A-domain	0.65 (0.03)	partial	202.4 (50.0)	hyperphosph.
A874V	A-domain	0.71 (0.02)	partial	162.1 (57.3)	hyperphosph.
R969Q	Loop 5-6	0.37 (0.00)	partial	291.4 (72.9)	hyperphosph.
P992L	P-domain	0.23 (0.03)	partial	129.0 (20.9)	normal
T1031S	P-domain	0.09 (0.03)	low	126.0 (57.9)	normal
P1052L	P-domain	0.02 (0.00)	no	90.7 (70.0)	normal
E1064K	N-domain	0.03 (0.01)	no	16.9 (11.0)	inactive
H1069Q	N-domain	0.13 (0.01)	low	51.4 (29.9)	inactive
L1083F	N-domain	0.22 (0.02)	partial	98.6 (25.1)	normal
G1213V	P-domain	0.03 (0.00)	no	119.8 (20.2)	normal
D1222V	P-domain	0.11 (0.02)	low	17.9 (6.0)	inactive
G1266R	P-domain	0.08 (0.01)	low	38.3 (35.3)	inactive
N1270S	P-domain	0.02 (0.02)	no	254.2 (126.9)	hyperphosph.
P1273L	P-domain	0.18 (0.01)	partial	245.6 (166.2)	hyperphosph.
S1362F-fs	TMD 8	0.17 (0.01)	partial	53.8 (13.2)	inactive
Human variants:					
S406A	NTD	1.08 (0.01)	normal	137.5 (45.1)	normal
V456L	NTD	0.50 (0.02)	partial	115.5 (58.2)	normal
K832R	A-domain	0.92 (0.00)	partial	130.0 (58.6)	normal

Figure Legends

Figure 1. (A) Catalytic cycle of ATP7B (the dotted frame highlights partial reactions, relevant for this study). (B) Transmembrane organization of ATP7B and representation of mutants and variants examined in this study. The six metal-binding sites in the N-terminal Cu-binding unit domain (NTD) of ATP7B are indicated by letters CxxC. ATP is bound to the nucleotide binding domain (N) and phosphorylated during ATP hydrolysis. The site of ATP-hydrolysis is the invariant residue D1027 (D1027A mutant = bold, arrow). The gene variants *S406A, V456L and K832R* are highlighted in italic. The CPC motif located in the sixth transmembrane domain is thought to form the intramembrane copper-binding site(s). A denotes the actuator domain.

Figure 2. (A) Copper transport by wt-ATP7B. Averages of ten independent experiments are shown. Copper uptake into vesicles was measured in nmol/mg protein over a time period of 240 min. Na_3VO_4 was added to the incubation solution to a final concentration of 200 μM (B) Mutation of the phosphorylation site of ATP7B (D1027A) abolishes Cu transport. (C) Copper transport by ATP7B mutants or (D) variants; Averages of three independent experiments are shown (mutants were selected to represent different functional domains; data for more mutants are shown in Table 1 and Supplementary Figure 2).

Figure 3. Phosphorylation activity of ATP7B mutants (A-E) and variants (F): The protein gels show representative ^{32}P autoradiograms of phosphorylated wt-ATP7B, variants and mutants. The phosphorylation activity (bar graphs) of variant and mutant ATP7B was

calculated in respect to wt-ATP7B activity (100%). Averages of 4-6 independent experiments are shown.

Figure 4. ATP-dependend dephosphorylation of the A-domain mutants (A) and P-domain mutants (B) of ATP7B at a copper concentration of 1 μM. ATP was added after [γ-^{32}P] ATP phosphorylation to a final concentration of 1 mM and incubated for 10 min at room temperature before the reaction was stopped. The typical gels and the phosphorylation activities of mutant ATP7B calculated in respect to wt-ATP7B activity (100%) for 3 independent experiments are shown.

Figure 5. Expression and localization of ATP7B mutants in mammalian cells. GFP-tagged ATP7B variants were expressed in HEK 293 T REx^{TM} cells. The expression pattern of wt- and mutant ATP7B is shown in the left column (green), organelle markers in the middle (red), and the superimposition of these images on the right (yellow). TGN46 is a TGN marker; Calnexin is marker for ER.

Figure 6. (A) Location of the characterized mutations in the functional domains of ATP7B. The structure of the P-domain was software-modeled using crystallographic structure of CopA (2B8E) as a template. For mutations within the N-domain, available NMR data (2ARF) were used. The NMR-based model for the A-domain was kindly provided by Dr. Lucia Banci. (B) Summary of key properties of ATP7B (left panel) that are affected by various mutations examined in this study (right panel).

Figure 1

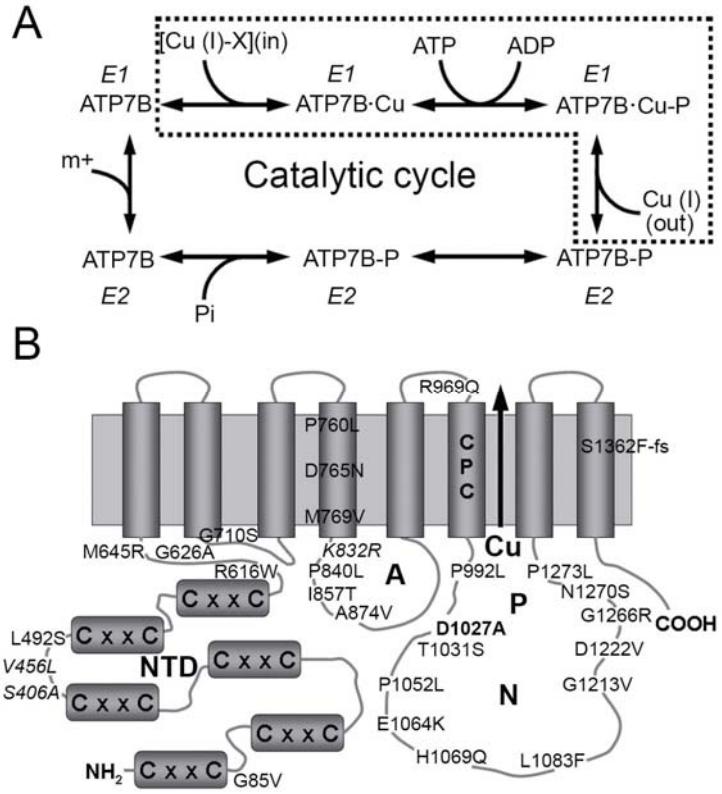

Figure 2

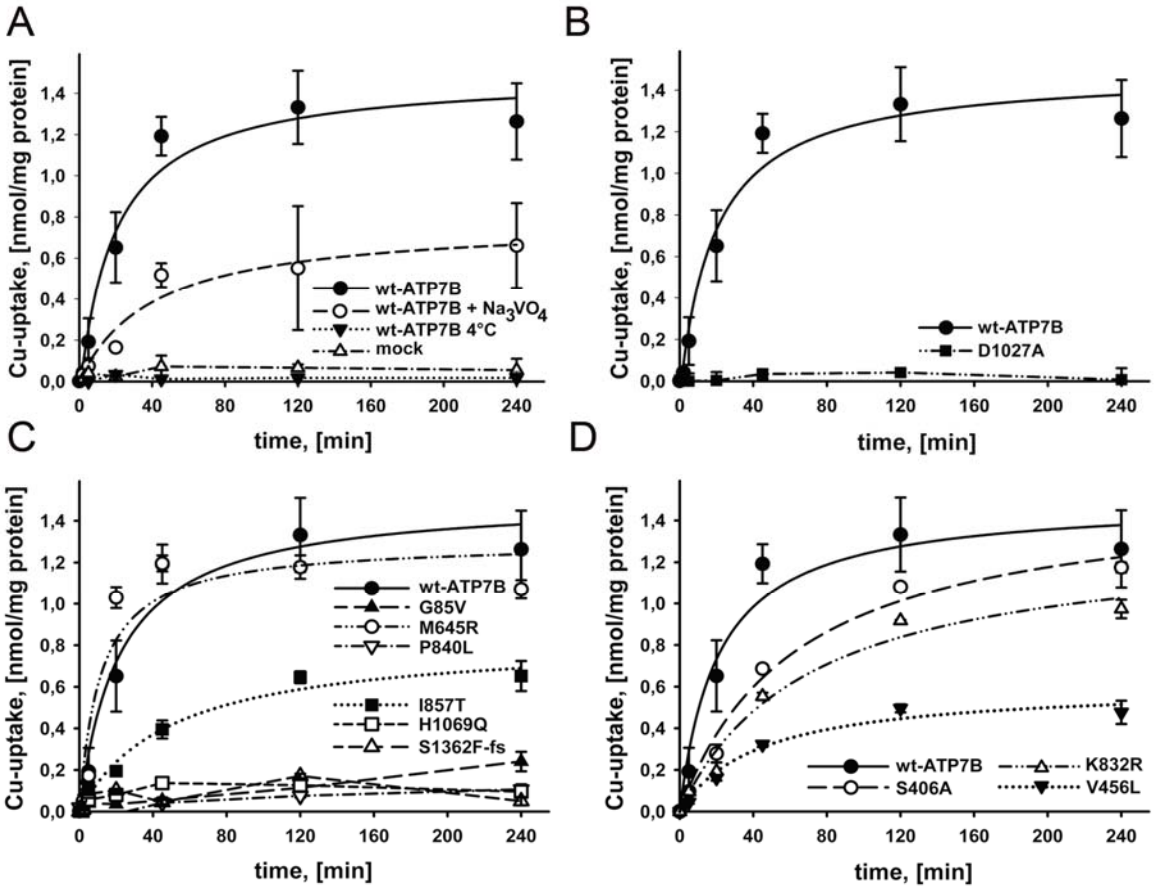

Figure 3

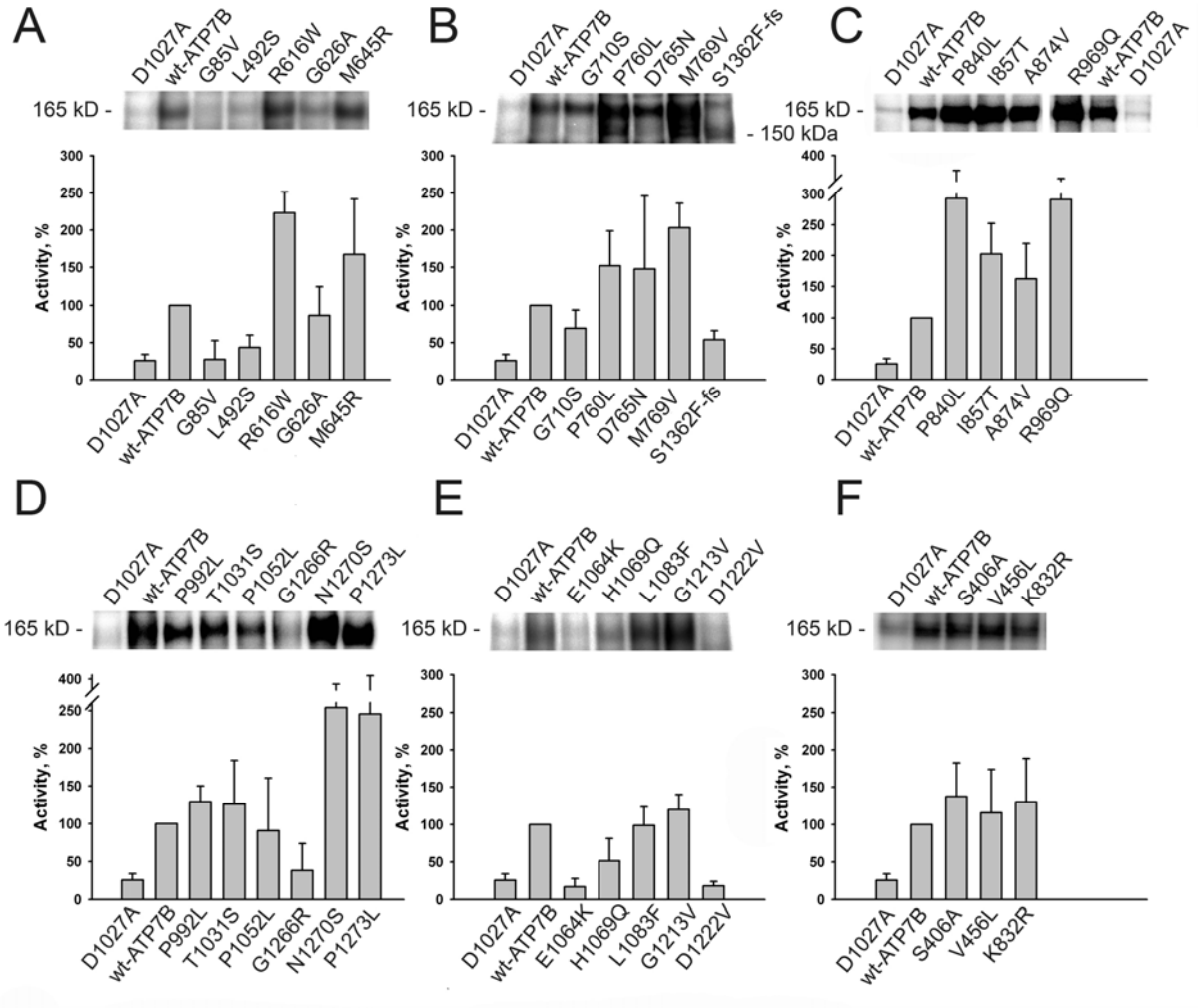

Figure 4

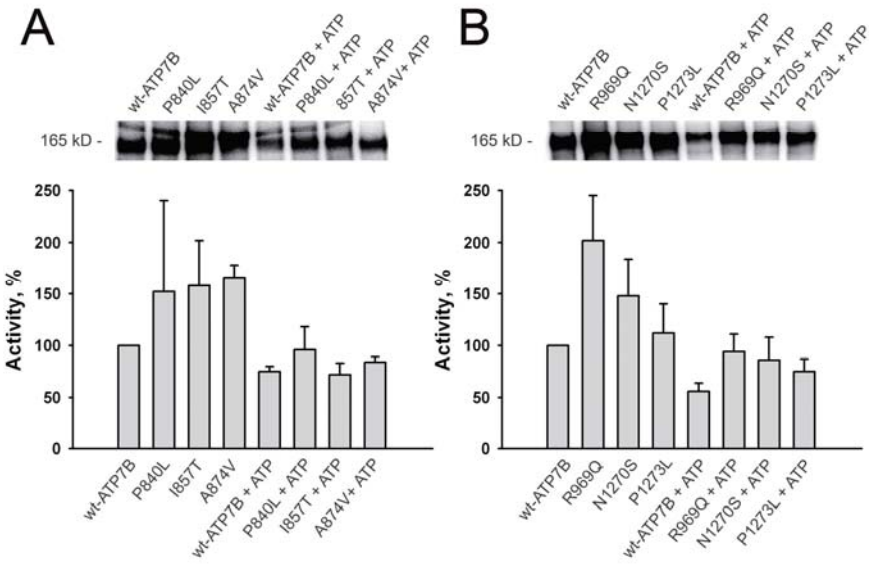

Figure 5

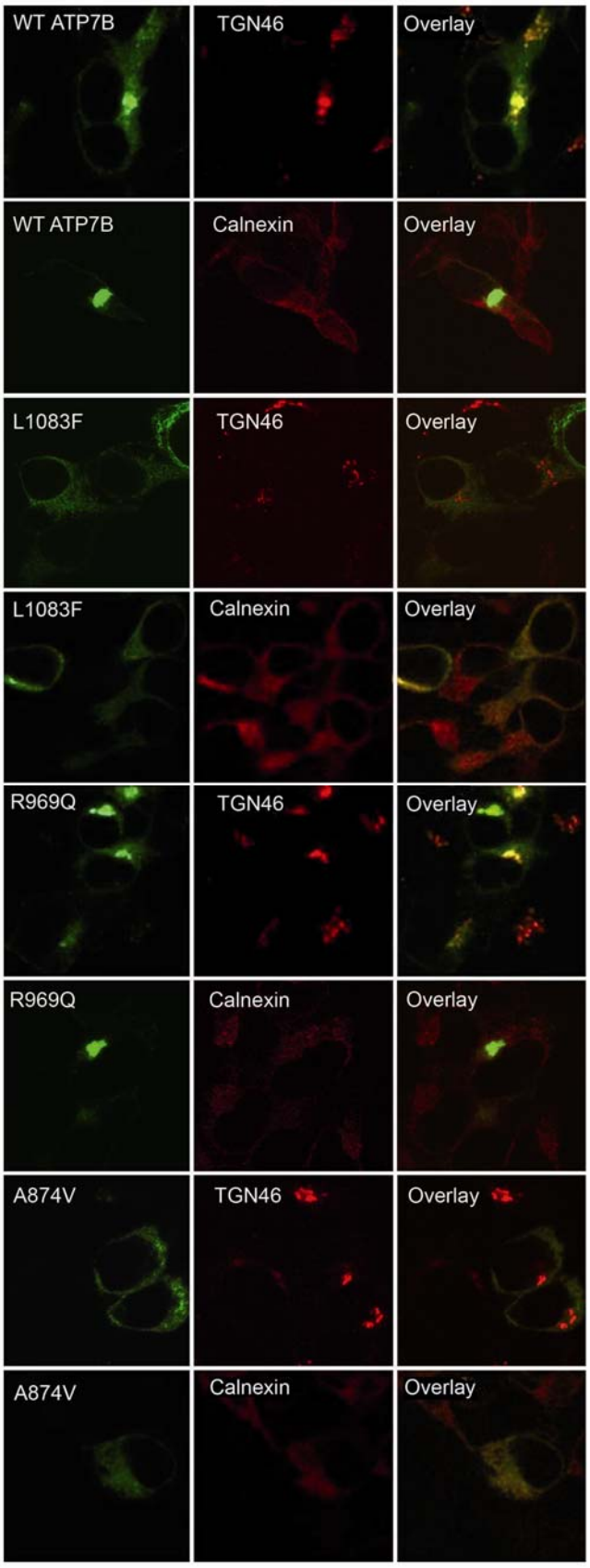
WT ATP7B
TGN46
Overlay
WT ATP7B
Calnexin
Overlay
L1083F
TGN46
Overlay
L1083F
Calnexin
Overlay
R969Q
TGN46
Overlay
R969Q
Calnexin
Overlay
A874V
TGN46
Overlay
A874V
Calnexin
Overlay

Figure 6